

Twitter Referral Behaviours on News Consumption with Ensemble Clustering of Click-Stream Data in Turkish Media

Didem Makaroğlu^{a,b,*}, Altan Cakır^{c,d} and Behçet Uğur Töreyn^b

^a*Demirören Teknoloji A.Ş., İstanbul, Turkey*

^b*Signal Processing for Computational Intelligence Group, Informatics Institute, Istanbul Technical University, Istanbul, Turkey*

^c*Physics Engineering, Faculty of Science and Letters, Istanbul Technical University, Istanbul, Turkey*

^d*Istanbul Technical University Artificial Intelligence, Data Science Research and Application Center, Istanbul, Turkey*

ARTICLE INFO

Keywords:

Click-stream
Social Media
Ensemble Clustering
Digital Media Industry

ABSTRACT

Click-stream data, which comes with a massive volume generated by the human activities on the websites, has become a prominent feature to identify readers' characteristics by the newsrooms after the digitization of the news outlets. It is essential to have elastic architectures to process the streaming data, particularly for unprecedented traffic, enabling conducting more comprehensive analyses such as recommending mostly related articles to the readers. Although the nature of click-stream data has a similar logic within the websites, it has inherent limitations to recognize human behaviors when looking from a broad perspective, which brings the need of limiting the problem in niche areas. This study investigates the anonymized readers' click activities in the organizations' websites to identify news consumption patterns following referrals from Twitter, who incidentally reach but propensity is mainly the routed news content. The investigation is widened to a broad perspective by linking the log data with news content to enrich the insights rather than sticking into the web journey. The methodologies on ensemble cluster analysis with mixed-type embedding strategies are applied and compared to find similar reader groups and interests independent from time. Our results demonstrate that the quality of clustering mixed-type data set approaches to optimal internal validation scores when embedded by Uniform Manifold Approximation and Projection (UMAP) and using consensus function as a key to access the most applicable hyper parameter configurations in the given ensemble rather than using consensus function results directly. Evaluation of the resulting clusters highlights specific clusters repeatedly present in the samples, which provide insights to the news organizations and overcome the degradation of the modeling behaviors due to the change in the interest over time.

1. Introduction

In recent years, the behaviors of the news readerships have shifted toward online channels after the digitization of news organizations and the rise of social media (Flaxman et al., 2016), which has a growing effect on consuming news. The importance of acknowledging the trend of news sources has been aroused by the news outlets which need to generate new revenue to adapt and survive in this era. Relatedly, the cruciality of the intermediaries has been recognized, and early researches have been focused on identifying the effects of these sources on attracting and holding consumers' attention by guiding users to new contents (Benlian, 2015; Chiou and Tucker, 2017; Dellarocas et al., 2013). Recent studies have shown that reaching news contents through social and nonsocial channels show different patterns (Möller et al., 2020), how news reader behaviours are formed with social (Facebook) and nonsocial media channel referrals at an aggregated level (Bar-Gill et al., 2021), how the readers spending time on the website and have the propensity to share the news differentiate by the referral channels (Köster et al., 2021). As a micro service, Twitter has become a key player in social media avenue and is used more than on aver-

age across 37 countries for reading, sharing, discussing news in Turkey (Yanatma, 2018). Strongly preferred as dissemination of the news, Twitter also mediates access to pages of news outlets. Considering that each social media site has different page structures, dynamics, and methods of influencing users, it is necessary to examine them separately to analyze the readers directed from these channels. To the best of our knowledge, the behavioral patterns of Twitter, as a social referring channel, have yet to be studied. In this paper, we delve into uncovering referred users' behavior by clustering methodologies. However, the readers tend to navigate away from social media and direct towards news websites with broad and diverse interests and intentions, making it hard to cluster for long periods. Therefore, we hypothesized and experimentally showed that working with separated data sets in this multidimensional environment is advantageous in recognizing and generalizing user patterns. By providing the distribution of the news category interests breakdowns of individual and general behaviors over time, we found that the behaviors are diverging over months; hence, working monthly data sets is beneficial in diminishing the volume and increasing the correlation within the samples.

2. Research Setting

The investigated data sets belong to Hürriyet, a news organization located in Turkey, founded in 1948 and is active not only on its website since 2004 but also promotes

*Corresponding author

✉ didem.makaroglu@demirorenteknoloji.com (D. Makaroğlu);
makaroglu17@itu.edu.tr (D. Makaroğlu); altan.cakir@itu.edu.tr (A.
Cakır); toreyn@itu.edu.tr (B.U. Töreyn)

ORCID(s): 0000-0001-9960-2113 (D. Makaroğlu); 0000-0002-8627-7689
(A. Cakır); 0000-0003-4406-2783 (B.U. Töreyn)

the contents and live broadcast in its social media accounts. In our one year period of analysis, between April 2019 to March 2020, the website had approximately 150M unique users and 300M visits per month. The traffic from the referral sites can be grouped as Social (Facebook, Twitter, Instagram, LinkedIn, Youtube) and Nonsocial (Organic -referred by Google-, other), with monthly visit shares 8% and 92% respectively, and Twitter has 25% of all social referrals. The objective of this study is to analyze referral users' behavior; thus, within this scope, our data sets include click-stream data, which is collected from the organization's website, and news content data. We limit our study with the collected data to uncover unsupervised behaviors of the referred users' patterns without comparing the findings with the nonsocial referrals, so this study measures neither the contribution of social referral users' behavior and news consumption on the website nor the causal effect of being directed to the news outlets (Mao and Zhang, 2015). This work presents a comprehensive methodology of ensemble clustering and explores different kinds of embeddings as input (i.e., UMAP) after experimenting with different sampling strategies (i.e., random, stratify). Our method evaluates performance metrics with clustering techniques to ensure behavioral clusters are stable and optimal within this structure. Furthermore, we provide a validation process to measure the similarity of the ensemble clustering with the optimal results. We evaluate the clusters generated by the selected clustering methodology over twelve months and show the behavioral patterns' stability and consistency in specific clusters.

The rest of the paper is organized as follows and can be followed from the given Figure 1 illustrates the framework of our system. Section 3 provides a discussion about related research on click-stream analysis and modeling, clustering with input data-types. Section 4 presents our data set, including collection and processing data platform, analysis of the distributions. Section 5 describes methodologies utilized in this work, including sampling and embedding strategies, ensemble clustering evaluation and comparisons, discusses the successful clustering. Finally, Section 6 concludes the article and presents our future work.

3. Related Literature

Click-stream data has been used to identify web usage and characteristics in many contexts (Catledge and Pitkow, 1995; Castellano et al., 2013). Clustering techniques are studied to utilize hidden user behaviours (Su and Chen, 2015; Wang et al., 2013; Grech and Clough, 2016a), related to this approach, unsupervised techniques are established to predict future groups (Zhang and Kamps, 2010). To identify the dominant behaviour groups, social networks and time-based frameworks are proposed (Lin et al., 2014), and enriched by having similarities to the group behaviour and individual propensities (Zheng et al., 2013). As news readerships have been studied in various approaches, recently, the research focus shifted to differentiating news consumption by considering the effects of referral channels (Möller et al.,

2020; Köster et al., 2021), and the intermediaries' power on algorithmic level (Thorson and Wells, 2016; Wells and Thorson, 2017). In our study, we also aim to find unsupervised readership behaviors for the specific referral channel Twitter, by using ensemble clustering methodologies without having neither ground truth nor predefined patterns in the data (Wang et al., 2016; Bogaard et al., 2019a).

As an unsupervised approach, for clustering user behaviors, there are different techniques, including centroid-based (K-means, K-Medoids)(Arora et al., 2016), hierarchy-based (Agglomerative) and density-based (DBSCAN (Schubert et al., 2017), HDBSCAN (McInnes et al., 2017)) partition. These algorithms have some advantages and disadvantages when considering some factors like scalability, time and space complexity, the ability to deal with categorical and numerical data types, noise and outliers. These algorithms need predefined values, including k numbers (K-means, BIRCH, Gaussian Mixture), epsilon value, and the minimum number of points (DBSCAN, HDBSCAN), linkage metrics including average, single, complete, or ward (Agglomerative). In recent years, Artificial Neural Networks have also been used for unsupervised clustering methods by applying auto encoders. One method is harnessed a deep auto-encoder architecture (McConville et al., 2021) we refer to as N2D, which takes advantage of deep neural networks to represent lower-dimensional data. With this method, after learning auto encoder embedding representations, UMAP(McInnes et al., 2020) is applied to better clustering with lower dimensions using local manifold learning. Similar to other clustering algorithms, this algorithm needs parameter optimization during model training and after reducing dimensions to form better clusters.

Ensemble methods have been proposed to overcome the limitations of clustering algorithms when used individually. The main purpose of these methods is to combine algorithms with relative deficiencies with appropriate methods and to apply various data set features or points with higher accuracy rates in a way that can capture the relationship between them. In the first step called Library generation, the aim is to obtain the set of clustering algorithms of m $K = \{K_1, K_2, \dots, K_m\}$ from data points in the D . It is revealed that the more the clustering algorithms in this method focus on various and different features, the more they can improve the contents of the clusters to be obtained by combining them at the consensus stage (Kuncheva and Vetrov, 2006). Thus, ensembling over a set of differences rather than similar labels will yield more efficient results. The K-means algorithm is generally preferred in the Library generation step because of its scalability and low complexity (Fern and Lin, 2008; Azimi and Fern, 2009; Alizadeh et al., 2014; Akbari et al., 2015; Pivdori et al., 2016; Yang et al., 2017). Among the methods used in this step are: getting results with different starting points or the different number of clusters with a single algorithm, working on samples with different data points or features, getting results on the same data points and features with more than one algorithm or combining several methods can be shown. In the consensus step, the K^* clustering algo-

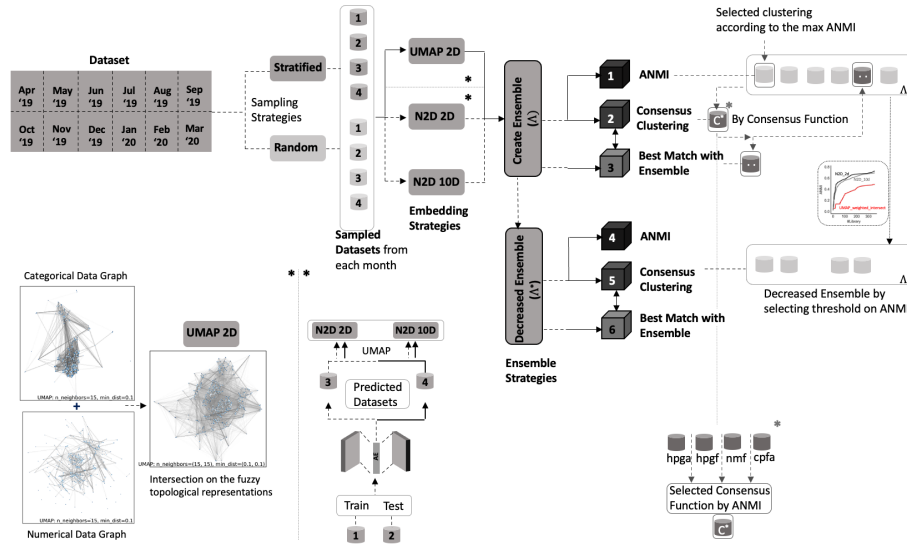


Figure 1: Methodology architecture. How N2D embedding strategies are prepared is shown at the bottom-left corner. With N2D embedding approach, 1st and 2nd samples are predicted by training on the 3rd and 4th samples. UMAP 2D is prepared by intersecting categorical and numerical features graphs as illustrated at the bottom-left corner for one sampled data set. The AAMI values are calculated for each consensus function result and then selected with the maximum value, shown at the bottom-right corner.

rithm, which will be used as the primary clustering method, is obtained from the cluster ensembles within the set of K by the consensus function. These functions are grouped under four main categories by (Boongoen and Iam-On, 2018) and can be listed as follows: direct, feature-based, pairwise similarity-based, and graph-based approaches, respectively.

To compare the performance of the clustering algorithms that are used in the consensus step, in this study, we followed the method (Helfmann et al., 2018) where new clusters are generated by consensus functions from predefined parameter space and compared accordingly. The algorithm procedure is described in Algorithm 1. The first strategy obtains the consensus by averaged normalized mutual information (ANMI) maximization. The second strategy comprise of two steps, at first the algorithm generates clusters by consensus function then finds the labels in the ensemble that shared the most information with the consensus step by the maximum normalized mutual information (NMI). It was shown that the optimal hyper-parameters found in the second strategy give at least the fitted result as consensus clustering K^* . Instead of a precise consensus function, in the last step, we applied the methods including Cluster-based Similarity Partitioning Algorithm (CSPA) (Strehl and Ghosh, 2002), HyperGraph Partitioning Algorithm (HGPA) (Strehl and Ghosh, 2002), Hybrid Bipartite Graph Formulation (HBGF) (Fern and Brodley, 2004) and NMF-based (Nonnegative Matrix Factorization) consensus clusterings (Li et al., 2007)) then selected the one which has the maximum AAMI score (see A.1). Although we have an ensemble of consensus function results, only the HPGA and NMF methods were resulted with the highest AAMI, and among these, the HPGA method was 95% more voted.

Algorithm 1: Hyperparameter search

Data: Data $D = \{x_1, x_2, \dots, x_n\}$ to cluster; Set K of ensemble clustering algorithms; Set T of consensus clustering algorithms

Result: Matched hyperparameter configuration with the selected consensus clustering

for $k \in K$ **do**

Find the clustering results $C(k)$ with the given clustering algorithm k for the investigated dataset;

Produce consensus clustering results from the given T ;

$t^{AAMI} = \arg\max_{t \in T} AAMI(C(t), T)$: Find the AAMI result of consensus clustering from produced clustering based on T .

return $k^* = \arg\max_{k \in K} AAMI(C(k), t^{AAMI})$

4. Observational Data Analysis

4.1. Design and Processing of Data Platform

Click-stream data sets are collected for the research period (April 2019 - May 2020) (Fig2), through web browsers by using AWS (Amazon Web Services; Elastic Beanstalk, Kinesis Data Streams, Kinesis Firehose, API Gateway, Lambda, S3, Redshift, EC2) technologies (Varia et al., 2014), which have been actively managing by the company, to enable elastic processing and storage for high-volume data. The collected real-time streaming data is combined and processed on Redshift, then stored on the S3 buckets, which can be accessed through both EC2 virtual machines and local environments. Content-based information collected and combined individually from company's servers

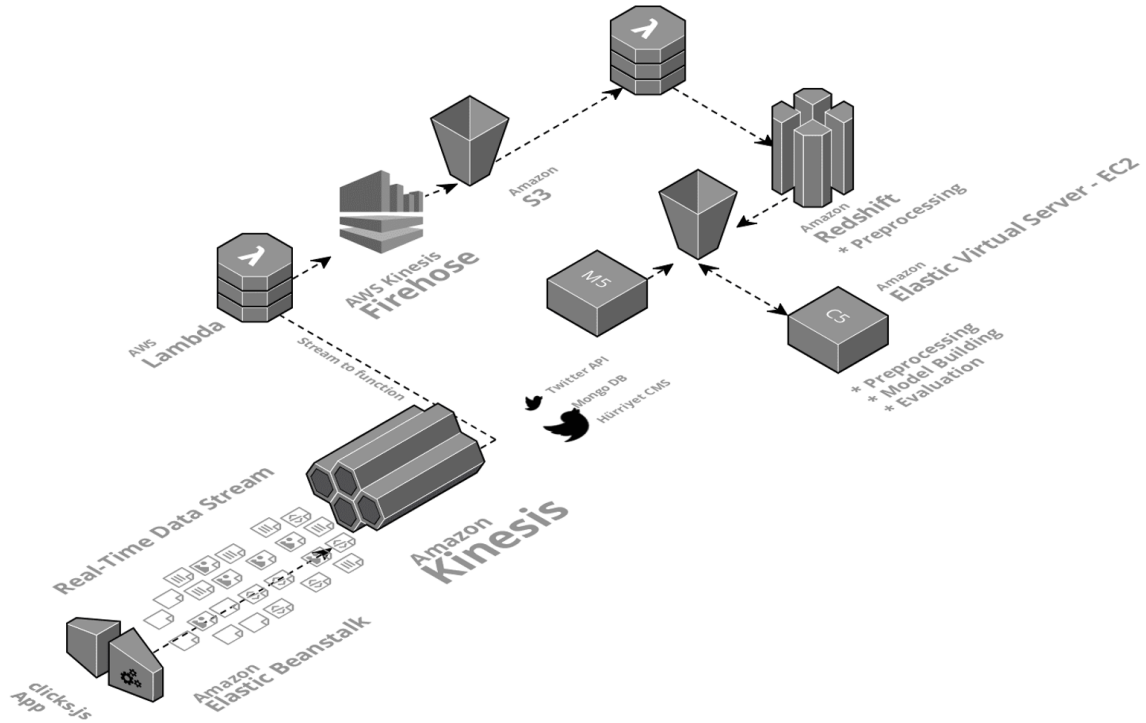


Figure 2: Click-stream data collection and preprocessing architecture on AWS (Varia et al., 2014). The click-stream data, generated by the readers' navigation actions on the website, and mainly the consecutive HTTP requests from a single IP address, are collected in the S3 buckets following the pipeline (from left to right): Hürriyet clicks.js application (collects each visit's action as a request from the website) → Elastic Beanstalk (is scaled up to 20 virtual machines to meet with traffic load) → Kinesis Data Streams (scaled up to 30 shards) → Lambda (to separate actions by referral types) → Kinesis Firehose → S3 → Lambda → Redshift (to provide large-scale query). The data sets are prepared on Redshift by querying and saved to S3 buckets. News content-based data sets (from Mongo DB) and additional sources are also collected on the S3 storages by EC2 virtual machines. Further analyses are processed on the EC2 virtual machines by reaching S3 buckets.

and AWS.

Click-Stream Data, stored in separated log files with a total size of 20TB of sequentially semi-structured format data for one year, belongs to the visitors' site history. An identification number (ID) is generated for each anonymized visit on the website, and the data spans these visits' navigation, including actions related to reading, time, browsing platform, content and location. The data set is aggregated to the each visit level such that a single entrance contains all articles read and content-based information included. As stated in the previous research (Makaroğlu et al., 2019) the distribution of total hourly visits referred from Twitter is similar to the hourly distribution patterns within Twitter when considered Hürriyet keywords. So, we deduce that the breakdowns of time-dependent distribution can shed light on the microservice usage patterns; with this inference, timestamps are expanded as *Hour, Week, dayoftheWeek*. The number of distinct articles accessed in a visit is represented as *VisitDepth* (the total number of contents), rather than embedding as sequential data. Twitter referrals are filtered from each visit's referring channel, and the rest of the data is excluded. The category of the articles are represented as categorical names e.g. travel, magazine, sports. Only *LeadCategory* is used during the analysis steps. The columnists' names of the articles also included in a single dimension.

sion.

Content-Based Data spans additional information about articles read by the visitors during the research, including *Postingduration* (Number of days between the date content is published on the website and the date of the visit), *NamedEntityRecognition(NER)* results (Aras et al., 2021) including *Person, Location, Organization*, and the daily *Contentsuccess* rank. Daily success ranks are calculated by scaling daily articles' PV scores within their category from 1(lowest) to 100(highest). We limit named entities according to the highest TFXIDF (Term Frequency x Inverse Document Frequency) scores within the scope of this study. The missing values in the categorical data types are not imputed; instead, they are represented in the data set as *unknown : UNK*.

After all the processing, the data set contains 5,666,125 visits originating from Twitter generated by 2,261,164 unique visitors, and includes the dimension as follows: *Hour, Week Number, Week Name, Month, Location (City, Country), Device (Mobile, PC), Visit Depth, Content Success, Posting Duration, LeadCategory, Columnist, NamedEntityRecognition(NER_P(Person), NER_O(Organization), NER_L(Location))*.

4.2. Analysis of LeadCategory Distribution

The first article accessed in the referred visit of the streaming data has a prominent role in leading readers from the social media environment and have a directed news consumption with more completion rates (Bar-Gill et al., 2021). Early studies showed that the interests in the news topics do change over time (Liu et al., 2010a). We thus examine the lead category's patterns by several breakdowns to show to what extent the distributions change, including browsing platform (to measure the effects of device preferences (Xu et al., 2014)), location and compare them with the general reading distributions over months. As described in the Section 4.1, each article's category information is included in the click-stream data with predefined topics, $c=\{'Sports','Current Affairs',...\}$. Category-level interests are formulated by dividing each category topic (c) with total clicks C_{total} that the user (u) made within the investigated month (m) such that the outputs given as a distribution vectors:

$$T(u, m) = \left(\frac{C_1}{C_{total}}, \frac{C_2}{C_{total}}, \dots, \frac{C_n}{C_{total}} \right) \quad C_{total} = \sum_i C_i \quad (1)$$

C^i is the total number of pageviews that the user made on the referred articles that is classified as the specific category for the given month. C^{total} is the total of these category pageviews. These distributions are found by considering individual anonymized user IDs as well as the *Overall* group of monthly readers. However, the referral IDs are vanishing at a great percent for each breakdown (Figure 3). A possible explanation for the observed differences in the rates of entrances is that the readers can systematically clear the IDs. To rule out this possibility, rather than tracking the individuals, we grouped them within discrete time windows, such that, in case the referral ID show up in one month, its group is defined as 1^{st} , if it is in two months then the group is defined as 2^{nd} , until the 11^{th} entrance in 1 year. Relatedly, overall monthly users' distribution is computed by dividing one year into 12 months and comparing divergence by grouping successor months as $1^{st}, 2^{nd}, \dots, 11^{th}$. JSD (Jensen-Shannon Divergence) metric (see Appendix A.1) is used to measure similarity with the given distributions. We obtain category-based characteristics by averaging each groups' JSD value. Figure 3, 4 depicts the lead category interests is differentiating across the grouped months and shows that overall months' distribution is more constant than individuals in all three breakdowns, including Mobile, PC, and City.

5. Methodology

This study utilizes an ensemble clustering evaluation method for patterns based on features extracted from readership browsing and content-based data. In Section 5.1, we explore different combinations of two embeddings as input representations (i.e., UMAP, N2D). In Section 5.2, we discuss the sampling approaches and evaluation of the selection of

the minimum sample size. In Section 5.3, we experimentally study to investigate ensemble clustering methodologies and evaluation of the optimal clustering methods. In Section 5.4, we discuss the results of the conducted experiments for the interpretation of reader behaviors stability that we obtained.

5.1. Embedding High Dimensions

When the correlation of categorical and numerical features before proceeding to the clustering step is below a specific value, the success in this step is affected as it can eliminate the redundant information during clustering. When we examined the correlation in all data types (numerical, categorical, ordinal), we observed that it changes within the limits of 0.2 to 0.75 over the months. Therefore, before proceeding to the clustering step, it is confirmed that none of the correlations found surpass the maximum cutoff that is 0.75. One Hot Encoding is applied for categorical data, and Power Transformation is applied for numeric data types. To make the numerical values more Gaussian-like, in this step, Yeo-Johnson's transform (Yeo and Johnson, 2000) is applied, which supports both positive and negative values and makes the data zero-mean while minimizing skewness. After the encoding step, we experiment two embedding representations named Uniform Manifold Approximation and Projection (UMAP)(McInnes et al., 2020) and N2D (McConville et al., 2021).

UMAP uses a graph-based approach to project the high-dimensional space to the lower dimension while preserving the global structure. L_2 norm for numeric values and Dice distance for categorical data types were used as distance criteria. As stated in the paper, with this method, we can generate fuzzy simplicial sets independently. UMAP supports intersecting two graphs and then embedding them as a consensus graph in low-dimensional space to create a single fuzzy simplicial set. The intersected graph neither has mostly dense areas as in categorical representation nor is weakly connected like in the numerical graph. Instead, it has the middle range of all connectivity placed by the probability of edge existence. To achieve this unity, we used percentages of categorical columns as weight parameters.

N2D lowers the dimensions by creating autoencoders with a trained neural network. After having a dense layer of created autoencoders, this method adds manifold learning to increase the clusterability performance by preserving local structures and capturing global structures. The article ((McConville et al., 2021)) states that if the total number of clusters in the dataset is known beforehand, the size in the UMAP stage should be defined as it is accordingly. In this approach, we compared the 10-dimensional, used in the original article to represent ten known clusters and the 2-dimensional UMAP results after learned autoencoders that we used in the first method as the final representation dimension of the dataset. Since our target is having a clustering $C = F_C(F_M(F_A))$; with better represented embedding space applied on dataset D with n data points in d dimensions $D = \{x_1, x_2, \dots, x_n\} \subseteq R^d$ in this approach we are in search of finding the most applicable clustering algorithm

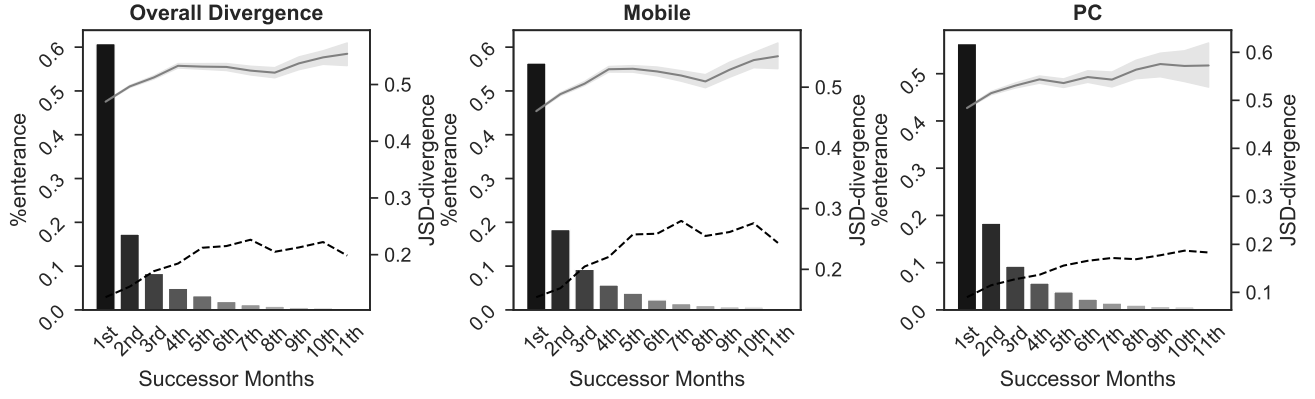


Figure 3: The comparison of Lead Category distribution by overall month (dashed black) and device types, including PC and Mobile (gray). The X-axis represents the group-level of entrances. The left Y-axis represents the rate of entrances within all data sets, and the right Y-axis shows the average of JSD values corresponding to the given groups.

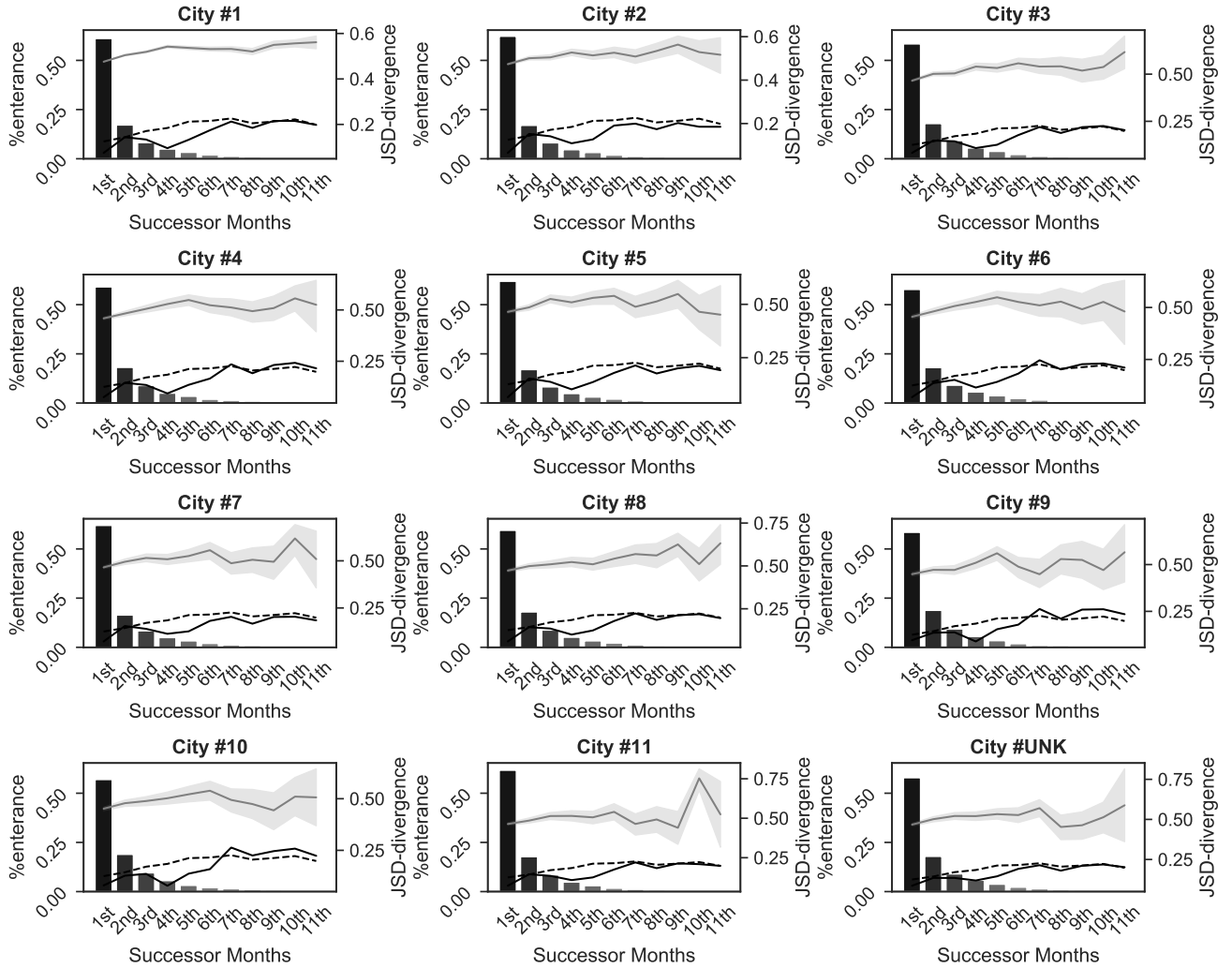


Figure 4: The comparison of City-level Lead Category distribution by overall month (dashed black), city-level month (black) and individuals (gray). The X-axis represents the group-level of entrances. The left Y-axis represents the rate of entrances within all data sets considering the investigated cities, and the right Y-axis shows the average of JSD values corresponding to the groups. The # numbers represent the different cities, which are positioned in descending order according to the total number of entries they have made during one year.

(F_C), after having a manifold learner (F_M) of autoencoder (F_A).

5.2. Sampling Approach

Most of the clustering algorithms' complexity is related to the number of sample data points. Therefore, it is both efficient and necessary to work on small-sized samples that can accurately represent the data, especially when working with large data sets. For this purpose, based on the results we obtained in section 4.2, where we observed that the interests of the users change over time by the news category, we select samples from each month to keep correlations among news interests as well as to include current news events that took place in that month and correlated with each other. Stratified sampling is an approved sampling strategy that captures the main characteristics from the given data set, is profoundly applied in large-scale data sets, and also gives high accuracy when sampled from the features (Jing et al., 2015). We compared different sampling strategies within the same months to observe the minimum sample size that we could proceed, including monthly behaviors. So, on the samples that we selected both at random and stratified by news categories from each month, the K-means algorithm is used to evaluate internal validation of the clusters, which is scalable and can return fast results. Silhouette coefficient (SI) (Rousseeuw, 1987), Calinski Harabasz index (CHI) (Caliński and Harabasz, 1974), Davies Bouldin scores (DB) and Dunn index-type (DI) (Dunn, 1974) measurements were compared by evaluating the number of clusters between 2 to 30 on four random and four stratified samples that we obtained from 5000 to 30000 in the increments of 1000 data points. To evaluate the clustering tendency of each sample, Hopkins test (Banerjee and Dave, 2004) is applied to the sampled data sets, which gave values close to 1 for highly clusterable data. According to the result of this test, if the values are close to 0.5, it is concluded that the data is distributed uniformly, and therefore clusterability is not possible. This value is found to above 0.95 for all sample sizes for the given months and as the sample size is increased, its clusterability also increases. Although the results of UMAP give lower values than the N2D approaches, especially for certain months, its clusterability is within the range of acceptable values that remain above 0.95.

5.2.1. Evaluation of Sampling by Internal Metric Validations

In order to evaluate the approach that the subsets of sampling strategies are related with each other, the similarity of each validation with the other results in its group is investigated. The Adjusted Mutual Information (AMI) (Vinh et al., 2010) (See Appendix A.1) score is computed during this evaluation because it could measure the success of the groups' association, regardless of the order of the labels and the sample size. An overview of this process can be found in Methodology 2. First, the metric scores correspond to the k values calculated concerning the selected sample size range in each month's random and stratified sampling strategies. After that, they were binned with the Freedman-Diaconis

rule (Freedman and Diaconis, 1981). While binning, each sampling strategy is evaluated between its minimum and maximum values in its primary group as random and stratified, so the results of different approaches are not suppressed by each other. After metric results are binned and labeled, AMI scores are calculated. To compare the validation information that a sample size shares with the sample group, the Averaged Adjusted Mutual Information (AAMI), which has proven success in ensemble methods (Strehl and Ghosh, 2002; Helfmann et al., 2018), is computed.

Methodology 2: Search of sample size

Data: Set K of cluster sizes; Set M of internal validation metrics; data $D = \{x_1, x_2, \dots, x_n\}$ to cluster; investigated sample range S

Result: AAMI of each sample size for the evaluated metric

forall $s \in S, m \in M, k \in K$ **do**

Find internal validation score for each metric m in the set of M correspond to the cluster size of k in the set of K, for selected s in the set of S ;
Scale the results between [0,1] within the given internal validation metric m ;
Bin the scaled results by FD rule within the given m ;

return $Bin_{FD}(Scale(M(s, m, k)))$ vectors for each range of sample size;

forall $s_i, s_j \in S_{i \neq j}$ **do**

$AMI(s_i, s_j)$;
Sum the AMI values for each sample s_i , that are calculated between each vectors of size $|K|$ for the given m for each sample;
Divide the Sum by the size of total range $|S|$ for each s_i to find average adjusted mutual information of the given sample s_i .

return $AAMI(s_i)$

One of the stratified sampling results from November is shown in Figure 5, except CHI, AAMI values relatively remain stable even the sample size is increased, which we expected to observe to set minimum sample size. Even though we used internal validity scores to determine the sample size, considering only the distance of the data points intra- or inter- clusters may cause non-convex geometries not to be detected, or this approach might not be meaningful for the cluster centers which are embedded in nonlinear sub-manifolds (Helfmann et al., 2018). The fact that any label cannot be known beforehand due to unsupervised learning problems confirms that we cannot use the external validity index in this problem where we aim to cluster user behaviors. For these reasons, we performed a knowledge-based assessment to confirm the stability of the resulting cluster in section 5.4.3.

5.3. Methodology of Ensemble Clustering

We applied the previous study's method (Helfmann et al., 2018) and referred to Strategy 1 and our approach to

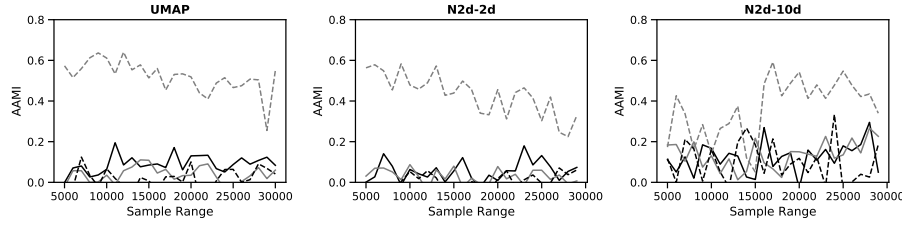


Figure 5: UMAP-2d, N2d-2d, and N2d-10d obtain AAMI Test results according to sample sizes. The colors in the graph lines represent applied internal validation metrics that are SI, DB, DI, and CH given in black, gray, dashed black, and dashed gray, respectively. One of the stratified samplings of November is selected for representation purposes. The X-axis represents the sample sizes increasing from 5000 to 30000. The y axis of the grid picture represents the AAMI values.

Algorithm	Time Complexity	Category
KMeans	$\mathcal{O}(kNT)$	Partitioning
Agglomerative	$\mathcal{O}(N^2)$	Hierarchical
Spectral	$\mathcal{O}(N^3)$	Model-Based
HDBSCAN	$\mathcal{O}(N \log N)$	Density-Based
DBSCAN	$\mathcal{O}(N \log N) \mid \mathcal{O}(N^2)$	Density-Based
Birch	$\mathcal{O}(N)$	Hierarchical
GaussianMixture	$\mathcal{O}(N'^2KD)$	Distribution
AffinityPropagation	$\mathcal{O}(N^2 \log N)$	Model-Based

Table 1

N: Number of samples, k: number of clusters, T: number of iterations, D: dimension

Strategy 2, which is shown in the model architecture in Figure 1. In the library step, we applied eight algorithms compiled with different parameters: KMeans, Agglomerative, Spectral, Birch, GaussianMixture, HDBSCAN, DBSCAN, Affinity Propagation. Therefore, the complexity of the Library step is the sum of the complexity of the algorithms (see Table 1). Once the Library step's clustering results are produced, their resulting clusters are found by applying four different consensus functions at the consensus step. The final consensus function is selected as the one which gives the maximum AAMI result among four different functions. For the final step of Strategy 1, the best match is selected by the maximum AAMI result given between the consensus function and the hyperparameter set of ensembles.

For the first step of Strategy 2, we consider clustering to be obtained with the consensus function, as explained in section 3, the higher the variance, the more accurate results can be extracted. To this end, a new ensemble set is obtained by sorting AAMI values from low to high and then eliminating those above a particular threshold value to reduce redundancy and complexity. Thus, clusters that produce similar labels are removed from the ensemble, and clustering is obtained with the consensus function among the remaining ones. As shown in Figure 6, when the AAMI scores of the relevant approach are sorted and observed according to the number of algorithms in the entire ensembles, it is revealed that both approaches have different threshold values. Regarding N2d, these values show similar patterns in 10- or 2-dimensional representations, which is stabilized earlier

than nearly half the value for UMAP. Considering that the AAMI results of different approaches have different distributions, threshold values of 100 and 200 are set for N2D and UMAP, respectively. After that, all steps in the Strategy 1 are applied to this new set. As a result, labels are obtained with six different clustering approaches for each data set.

5.4. Evaluation

5.4.1. Clustering Results

The primary purpose of clustering validation is optimal discrimination among reading behavior groups, which would help newsrooms recommend specific news for those in the given clusters. Since we have 6 different strategies with all consensus clustering labeling, there are 356 possible clustering solutions in total. Therefore, the evaluation of the resulting clustering is nontrivial for this study since there is no ground truth available in the data and also the knowledge-based interpretations are subjective. Consequently, in the first step, we aimed to reach the most optimal evaluation results among clustering approaches. In order to identify successful strategies, internal validation metrics (SI, CH, DB, SDbw (Halkidi, Kim, Tong))(see Appendix A.1) are compared based on the results of the clustering algorithms obtained for the month, embedding and sampled data set. With this, we could observe both compactness/separation and arbitrary shape density validation of the clusters. As stated in the previous study (Handl et al., 2005) internal validation metrics must be selected by the applied clustering algorithms since both of them are considering the underlying structure of the given data set. So, the metrics, especially when the ground truth is not known, are crucial for validating the resulting clusters. As reviewed in the study (Wegmann et al., 2021), metrics also come from certain assumptions, so there is a trade-off in the choice of these evaluations. In the given review study, cluster validation evaluated under four main categories: Cluster(shape(spherical/convex, non-standard geometry, arbitrary) and numbers(can be biased to the high number of clusters)), Handling Noise (ability to deal with outliers without preprocessing) and Computational cost/complexity, on the other hand, capability with sub-cluster identification, skew distribution also evaluated by another study (Liu et al., 2010b) (See Table 2). Therefore, we evaluated cluster performances in a format that included various validation perspectives, as different characteristics

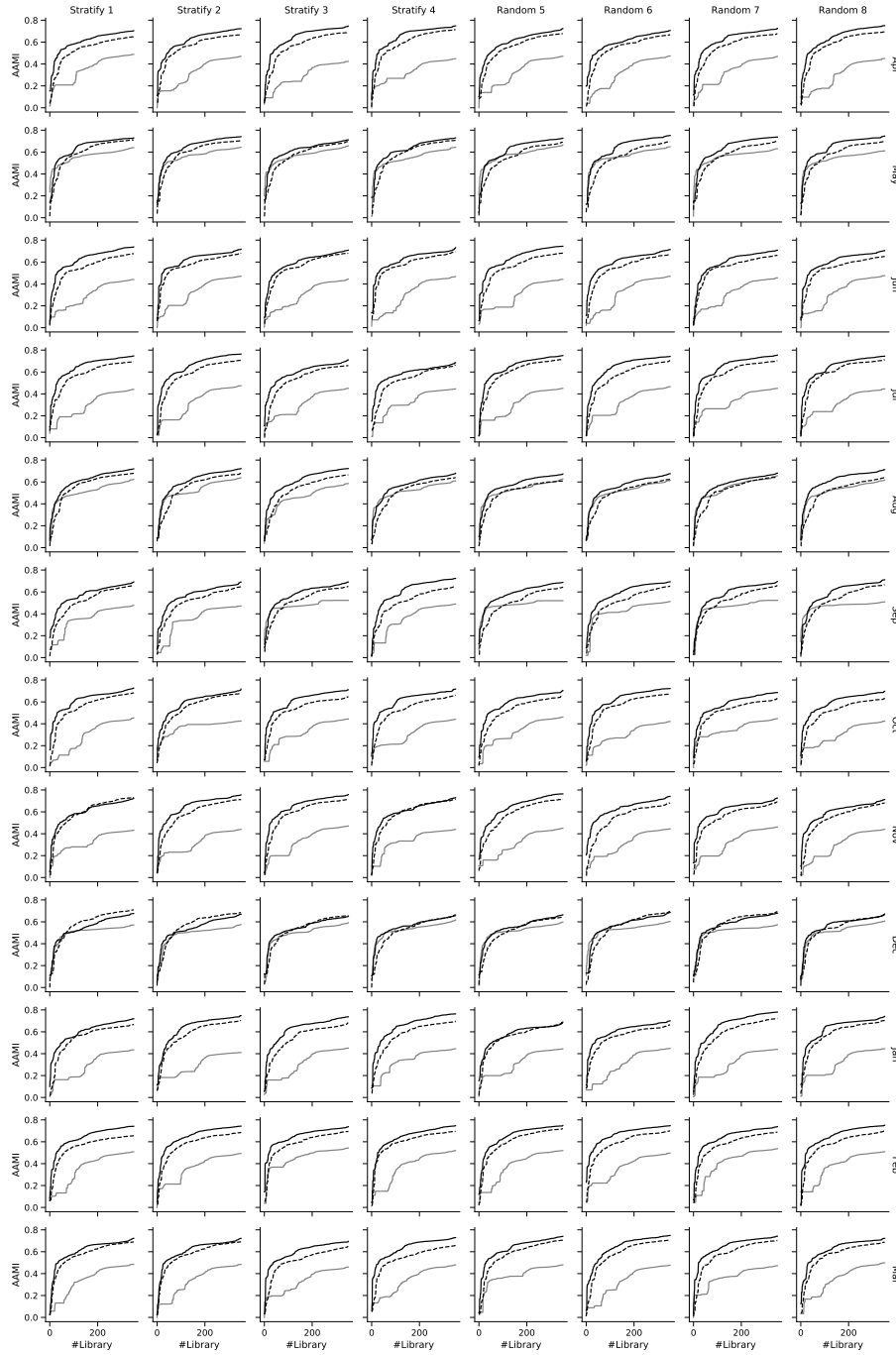


Figure 6: AAMI results are obtained after decreased ensemble approach. The colors in the graph lines represent applied embeddings that are UMAP, 10-dimensional N2D, and 2-dimensional N2D given in gray, dashed black, and black, respectively.

of clusters could be focused on.

Internal validation values are used as a measure to determine the optimality as the quality of clusters, which gives successful results in the previous study on identifying behaviors (Rodríguez-Fernández et al., 2017). Following this purpose, internal validation metrics of the clusters formed by the algorithms within the ensemble groups created separately by Strategy 1 and 2 are evaluated. Considering the optimal value of the metrics at the minimum and maximum limits, all scores are unit-based scaled between [0,1] within

the evaluated data set. Then the successful metric was decided according to the one with the highest variance among these lists. As shown in Fig 7, although there are standard metrics, the majority of the selection belongs to CHI(%76) among all, the rest of the top selections are Sdbw(Kim)(%8), SI(%7), Sdbw(Halkidi)(%5), Sdbw(Tong)(%4), respectively. The algorithm classes which take the best values in the limits of the metrics with the maximum variance are shown in the Fig 8. According to the results, while the most successful algorithm for CHI is Kmeans, HDBSCAN did not give any

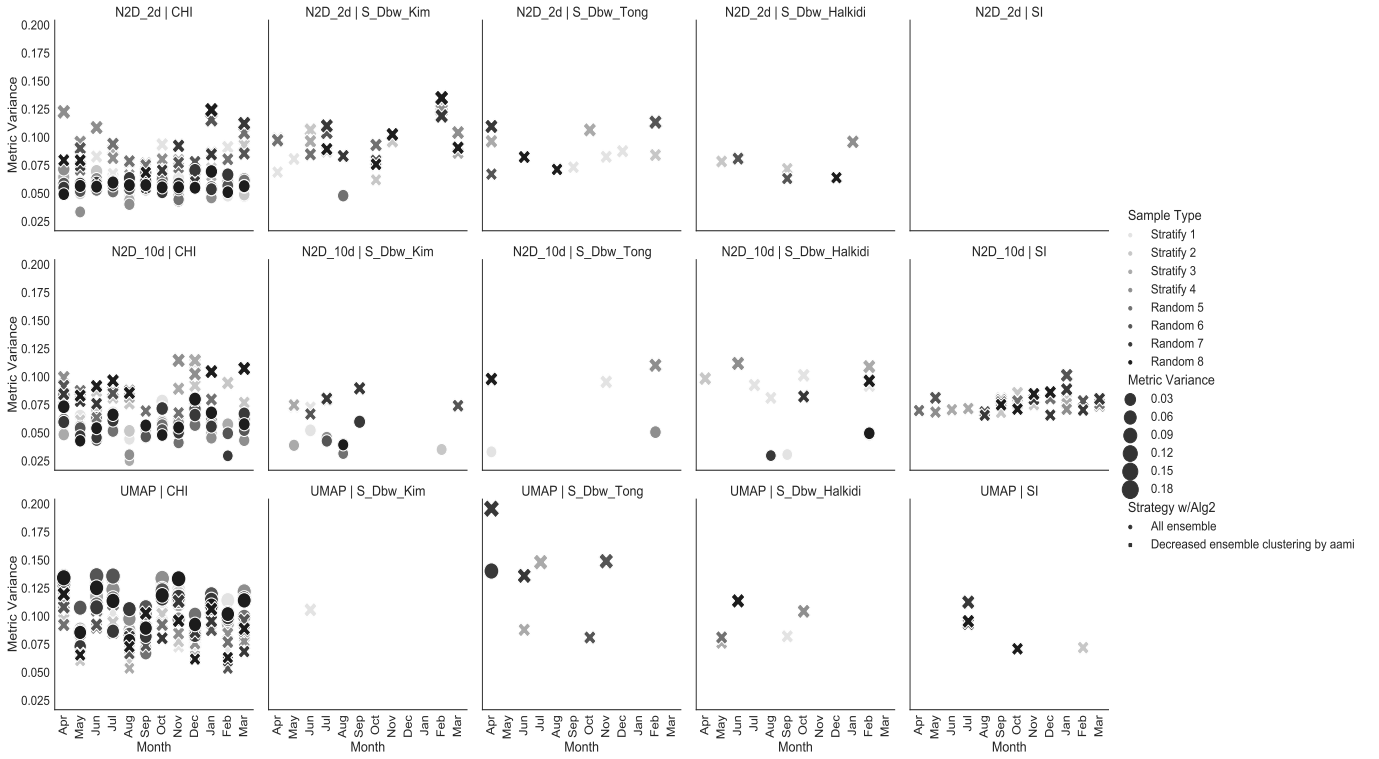


Figure 7: Metric selection by individual data sets sampled from each month and applied different strategies to embeddings. Cross sign "x" represents the optimal Library metric results according to the Decreased ensemble Library, and sphere "o" represents entire ensemble set.

Table 2
Evaluated metrics' comparison

Metric	#Cluster Bias	Handling Noise	Sub Clusters	Skew Distribution	Optimal Value
SI	No	Depends on Noise(%)	No	Yes	Max
CHI	No	No	Yes	No	Max
DB	No	Yes	No	Yes	Min
Sdbw (Halkidi)	Yes	Yes	Yes	Yes	Min
Sdbw (Kim)	Yes	Yes	Yes	Yes	Min
Sdbw (Tong)	No	Yes	Yes	Yes	Min

results with CHI, which gets the best validation scores with Sdbw. So, this result also supports the internal validation approach of Sdbw that considers density area in the selected cluster.

5.4.2. Selection of Successful Strategy

To select the successful embedding and strategy, we utilize the closeness of the strategies and embedding approaches to the optimal metric scores. Although the CHI metric is found to give a generalizable result, it has been observed that different metrics can give optimal results in

some months due to the differences in the distributions of the monthly data set samples. For this reason, the metric values obtained with the strategies and approaches are evaluated with a filtering approach as described in the steps that can be found in Table 3.

1. At first, the algorithms, which are given by the metrics obtained according to the maximum variance calculation, are extracted (Optimal/Metric). Then, considering the optimal value of the metrics at the minimum and maximum limits for each breakdown, the top 5 results with the best score are obtained and ranked between 1(the best) to 5(the least). Thus, optimal metrics giving the best five scores for Strategy 1 and Strategy 2 and algorithms providing these metrics (Optimal/Algorithm) are prepared.
2. The closeness of the applied strategies' metric scores are calculated by taking the differences of the optimal metric values, which can be selected differently from CHI according to the data sets, and the corresponding metric values of the applied strategies on that dataset. The value differences are then scaled within the observed metrics between [0,1], 0 represents the closest to the optimal value, while 1 means the farthest (Evaluation/Closeness). 1 is the closest to the optimal value.
3. The top 5 optimal algorithms filtered in the first step are compared with the algorithms obtained with the strategies and weighted their performances with spe-

Twitter Referral Behaviours in Turkish Media

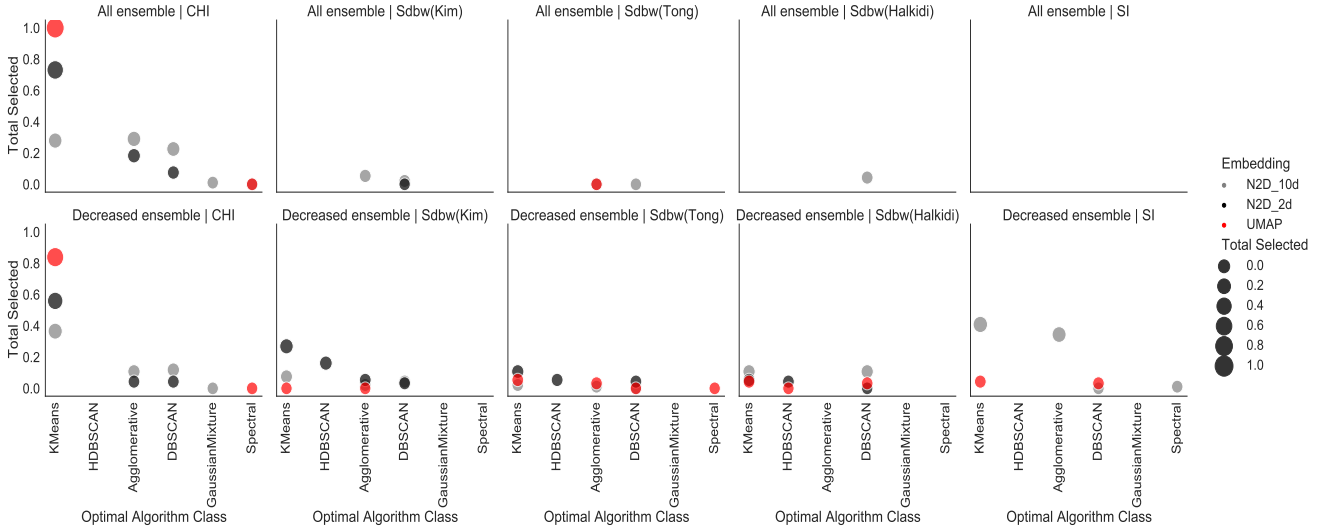


Figure 8: Optimal metrics obtained according to the maximum variance selection and algorithms that take their values at the maximum limits of these metrics. While the columns show the selected metrics, each strategy groups are represented in the rows. Embedding breakdowns are discriminated by the colors.

cific coefficients. These coefficients are determined so that if an exact match with the algorithm (including all hyperparameters) occurs (Evaluation/Exact Match), the optimal algorithm's rank is (1-5) placed, and if not, the minimum value (6) is placed (Evaluation/Rank Weighted). We evaluated the closeness of the clusters formed by the consensus function to the optimal algorithm with the ranking value obtained by the Hyperparameter Match method, since there can be no match with any optimal algorithm in the consensus step. Because the clusters obtained as a result of consensus, the algorithm with the highest similarity to the library is found by the Hyperparameter Match method. Therefore, this similarity gives us the similarity of the consensus result to the optimal values (Evaluation/Rank Weighted, in red). However, we observed that the internal validation scores of the optimal algorithms on the samples give more successful results than the clusters obtained by consensus.

4. The scaled closeness values, which are obtained in the second step, are multiplied with the coefficients obtained in the third step (Evaluation/Rank Weighted * Evaluation/Closeness = Evaluation/Weights). Then based on each sample, the results are ranked between 1 (the best) to 6(the farthest) (Evaluation/Rank). Therefore, considering the entire data set, the embedding approach with the highest number of times ranked 1 is the closest to the optimal value.

The successful strategy is found by following the applied embedding considering the ranking criterion given in the Evaluation/Rank column (Table 3). Thus, the results are ranked from minimum values to give the closest result to the optimal value and the maximum values to give the farthest result. At the same time, the performances of strategies that can achieve one-to-one matches were also weighted. In this

step, we also discriminate the rankings as stratified and random to compare the sampling types.

As illustrated in Fig 9, even there are rank one results and one-to-one matching algorithms with optimal algorithms of N2d-10d and N2d-2d embeddings, the closest approach to the optimal algorithm is Hyperparameter Match Strategy 1 with UMAP embedding, which has the highest number of selection in rank 1. Based on these results, we conclude that the Hyperparameter Match Strategy 1 with UMAP result is the closest approach to the optimal values. Additionally, we conclude that the CHI metric produces the best quality clusters compared to other metrics. When we compare sample types, we can say that stratify, and random sampling mostly show similar behaviors, which may be due to the solid semantic correlation of the data sets within months.

5.4.3. Cluster Stability

The stability of the clusters is defined as the reoccurrence of the resulting clusters in different periods, even when the data points change. Some previous researches applied this procedure by having frequent samples without replacements and averaging the similarities with Jaccard coefficient (Grech and Clough, 2016b), another study investigated this approach to compare similarity between monthly samples of a digital library (Bogaard et al., 2019b) which concludes that there is a trade-off between silhouette width and the stability scores of the clusters. Our study validates the stability of resulting clusters in separated months by computing the average AMI scores to indicate clustering quality, which also mean these clusters are the general reading behaviors of the users whose referral channels are Twitter.

Cluster Distributions: In order to determine the stability, the distribution of the features in the clusters is obtained

Twitter Referral Behaviours in Turkish Media

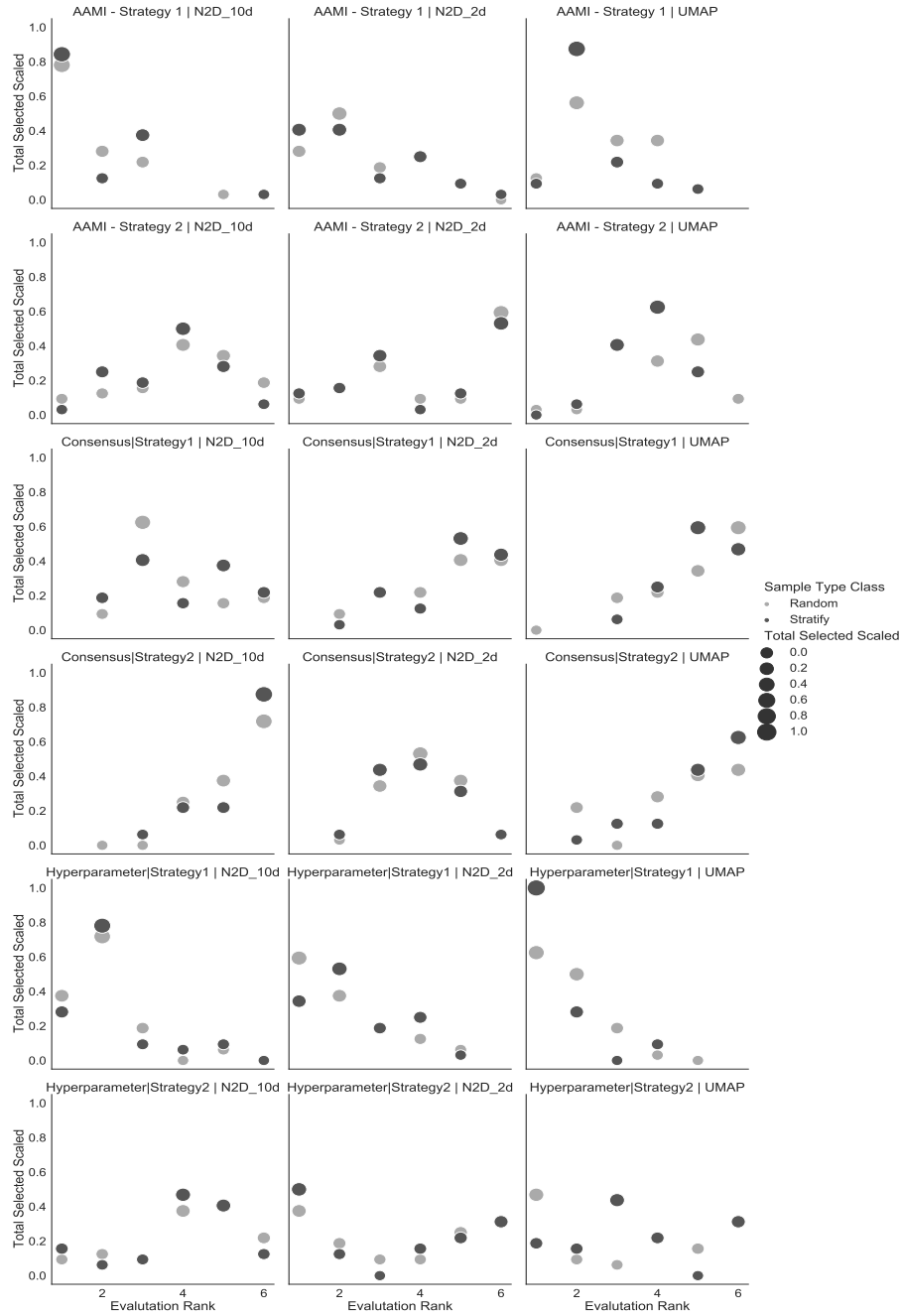


Figure 9: This figure shows the closeness of the metric scores obtained with the applied strategies to the optimal metric scores, which are selected individually for the sampled dataset and ranked according to the filtering approach. Each embedding is represented in columns: N2D-10d, N2D-2d, UMAP. While the columns show the embeddings, each strategy applied is represented in the rows. Stratify and random sample types breakdown are discriminated in black and gray colors, respectively. Each chart includes rankings from 1 to 6 on the X-axis, while the Y-axis shows the total selections of these rankings during the year. The choice closest to the optimal metric value shows the approach and strategy with the highest total selection value in the 1st rank in this chart.

in each sample as in 2.

$$F_1^1 = \left(\frac{f_1}{C_1}, \frac{f_2}{C_1}, \dots, \frac{f_i}{C_1} \right) \quad C_1 = \sum_i f_i \quad (2)$$

For each cluster the distribution vectors of feature's values are computed. So if there are n number of features in

the first cluster C_1 , the dimension can be shown as $F = \{F_1^1, F_1^2, \dots, F_1^n\}$. For feature F_1 , there are a certain number of times the unique values f_i in this specific feature are placed in the given cluster C_1 . The total size of this feature will be equal to the total size of this cluster C_1 . So the distribution of F_1 in the first cluster C_1 can be found as F_1^1 .

Fig 10 shows, per cluster, that have more than 0.5 AMI

Table 3: Clusters with the highest reoccurrence counts

Strategy, Dataset, Approach				Optimal				Selected			Evaluation				
Month /Sample	Embedding	Strategy w/Alg	Strategy	Class	Hyper-parameters	Metric Value	#Clusters	Hyper-parameters	Class	#Clusters	Exact Match	Closeness	Rank Weighted	Weights	Rank
May /Random 6	N2D_10d	DE	CC- Sig 2	Agg	L2_Avg_2	SI - 0,662	2	hgpa	HGPA	163	0	0,56	6	3,34	6
			HM - Sig 2					KMeans	4	0	0,32	6	1,93	5	
			ANMI - Sig 2					Euc_comp_14	14	0	0,09	6	0,47	1	
	UMAP	AE	CC- Sig 1	KMeans	k = 30	CHI - 8459,528	30	hgpa	HGPA	290	0	0,23	6	1,40	4
			HM - Sig 1					L1_15_0,8	68	0	0,21	6	1,28	3	
			ANMI - Sig 1					Euc_avg_26	26	0	0,09	6	0,51	2	
		DE	CC- Sig 2	KMeans	k = 30	CHI - 13293,156	30	hgpa	HGPA	163	0	0,37	6	2,20	5
			HM - Sig 2					Euc_15_20	63	0	0,37	6	2,24	6	
			ANMI - Sig 2					L1_Avg_10	10	0	0,20	6	1,23	3	
		AE	CC- Sig 1	KMeans	k = 30	CHI - 13293,156	30	hgpa	HGPA	250	0	0,34	6	2,04	4
			HM - Sig 1					Birch_30	30	0	0,13	6	0,77	1	
			ANMI - Sig 1					Euc_avg_24	24	0	0,14	6	0,83	2	
N2D_2d		DE	CC- Sig 2	KMeans	k = 30	CHI - 9998,848	30	hgpa	HGPA	163	0	0,27	6	1,63	5
			HM - Sig 2					L2_15_10	112	0	0,27	6	1,62	4	
			ANMI - Sig 2					L2_20_20	80	0	0,28	6	1,67	6	
		AE	CC- Sig 1	KMeans	k = 30	CHI - 9998,848	30	hgpa	HGPA	276	0	0,28	2	0,55	2
			HM - Sig 1					Agg_ward_30	30	1	0,00	2	0,00	1	
			ANMI - Sig 1					Agg_euc_avr_28	28	0	0,15	6	0,88	3	

Abbreviations used in the table: Strategy/Alg Decreased Ensemble: DA, All Ensemble: AE, Consensus Clustering: CC, Hyperparameter Match: HM, Averaged Normalized Mutual Information: ANMI, Strategy: Sig, Hyper-parameters: Complete: comp, Average: avg, Euclidean: Euc, Class: Agglomerative: Agg

values according to 2 when compared with the rest of the clusters in all months that are labeled as high stability. Since NER attributes are mostly related to the given text of articles, they are compared by including and excluding these features. The results show that the highest stability counts can be obtained without NER attributes with average stability of 10 out of 12 months. For example, in the Hyperparameter Match strategy, while 1 cluster obtained from April have matching clusters in June with NER included, the results increased to 4 when NER results are excluded.

Table 4 represents the characteristics of the clusters belonging to the specific month, which are reoccurred at the highest rate in other months. The observations of these clusters can be summarized as follows:

- In particular, the recently published articles that bounced from the first news referred to in *City1* are stable for all clusters.
- The clusters with the highest volume could not achieve the similarity threshold with any clusters; instead, when we observe over months, the stability of the resultings is high, with a minimum rank of 4 and a maximum of 20 among all.
- The entertainment category is primarily read in the afternoon with mobile devices.
- While Weekday readers are reoccurred over the months, the weekend readerships do not have high stability rates.
- The clusters that have columnists are higher ranked articles than other categories.
- While Mobile users are the majority among the device selection, PC users are mostly reading Current Affairs with political issues.

6. Conclusions and Future Work

Based on the detailed click-stream data, this study reveals the reading pattern of the anonymous readers whose referral channels are Twitter. Users' reading characteristics are first analyzed by *leadcategory* distribution over months by location and device breakdowns, demonstrating that the underlying distribution diverges over time. Ensemble clustering analysis is utilized by comparing different embedding approaches and strategies on methodologically selected samples to identify stable clusters independent from time. Since the methodologies are applied based on the data by one news outlet, Hürriyet, may cause the results not generalizable; thus, we conduct the stability analysis over the months, which yields profoundly stable patterns. The prominent characteristics of these findings show that some of the columnists have a substantial and continuous impact on directing the readers to the website. Mostly low ranked news is found to be directed, but when it comes to the columnists and rarely directed locations, the behaviors change mainly to

Twitter Referral Behaviours in Turkish Media

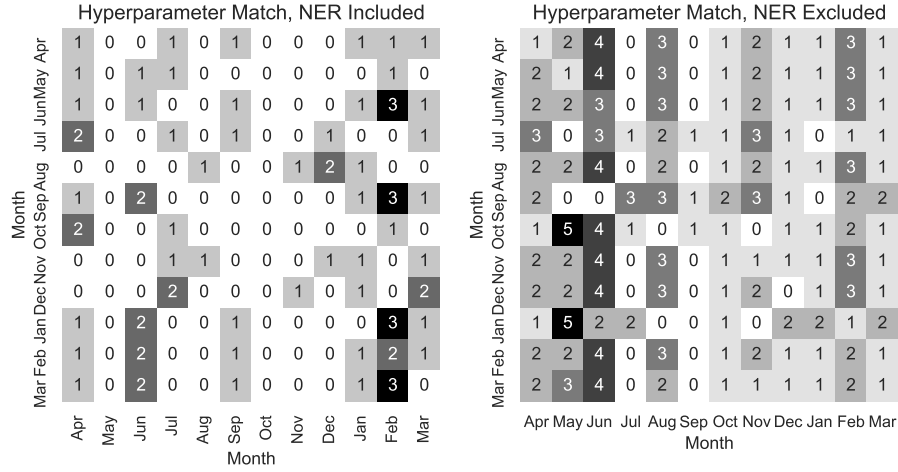


Figure 10: Comparison of all features' distributions over the all clusters with AMI. Left figure includes NER results, which are excluded from the right figure.

Table 4
Clusters with the highest reoccurrence count for a specific month

Month	Apr	May	Jun	Jul	Aug	Sep	Oct	Nov	Dec	Jan	Feb	Mar
Cluster Size(%)	4,36 - 6	2,84 - 20	5,87 - 4	2,4 - 19	3,98 - 12	2,19 - 20	4,38 - 10	4,4 - 9	4,35 - 11	5,69 - 4	2,42 - 24	4,33 - 8
Rank												
#of Reoccurrences - Unique Months	19 - 10	19 - 10	19 - 10	17 - 10	19 - 10	19 - 9	18 - 10	19 - 10	19 - 9	18 - 9	19 - 10	18 - 10
Algorithm - #of Clusters	B - 30	B - 26	A - 30	B - 30	B - 30	A - 30	A - 30	A - 30	B - 20	A - 30	A - 30	A - 30
Bounce(%)	86.7	97.18	93.9	94.17	95.98	92.66	89.55	80	73.73	55.48	90.91	96.77
City1(%)	44.95	44.37	41.69	47.5	46.73	43.12	48.18	40.91	47.93	48.76	41.32	45.62
Recently Published (%)	97.25	93.66	99.66	98.33	95.98	95.41	86.82	98.64	98.62	98.23	28.1	60.37
Ranking(%)	LR - 78,9	LR - 40,14	MR - 68,47	MR - 31,67	LR - 43,72	LR - 41,28	LR - 45,45	LR - 41,82	LR - 36,41	LR - 33,22	LR - 97,52	LR - 97,24
Category(%)	CA - 63,3	E - 71,13	C - 56,95	C - 35	Et - 91,46	CA - 59,63	CA - 29,09	Et - 32,27	CA - 89,86	CA - 79,86	Et - 33,88	T - 38,71
Device(%)	M - 59,63	M - 97,89	M - 70,85	M - 75,83	M - 85,43	M - 82,57	M - 57,73	PC - 76,82	PC - 94,01	PC - 78,8	M - 87,6	M - 82,49
Hour(%)	AN - 9,63	AN - 11,27	MR - 13,22	MR - 21,67	AN - 13,07	AN - 17,43	MR - 14,09	AN - 14,09	MR - 12,9	AN - 14,84	AN - 10,74	MR - 15,67
NER(%)	IP - 17,4	UNK - 46,71	P - 26,44	P - 13,33	EtS - 63,82	UNK - 42,81	None - 21,6	UNK - 22,12	UNK - 10,6	P - 13,07	IP - 18,18	UNK - 59,44
Weekday(%)	39.45	42.25	26.1	49.17	26.63	56.88	25.45	34.09	23.5	80.21	40.5	39.63
Weeknumber(%)	1st - 78,44	3rd - 78,17	2nd - 98,64	3rd - 58,33	4th - 100,0	4th - 96,33	2nd - 46,82	2nd - 33,18	4th - 96,31	4th - 50,18	3rd - 70,25	2nd - 60,37

Abbreviations used in the table: *Algorithms* Agglomerative: A; Birch: B; *Rank* Low Rank: LR; Mid Rank: MR; *Category* Current Affairs: CA; Economy: E; Entertainment: Et; Travel: T; *Columnist*: C; *Device* Mobile: M; *Hour* Afternoon: AN; Morning: MR; *NER* City1 - Politics: IP; Unknown: UNK; Politics: P; Entertainment show: EtS

the high ranked contents. In general, morning readers have the majority, but entertainment news is mostly read in the afternoon. The latest generated news is preferred primarily by the readers, with that we can deduce the readers are most interested in the trending news.

Our empirical analyses with a comprehensive perspective of the clustering methodologies could find stable reading habits, leading to a number of further investigations. Our first plan is to reduce complexity and increase the robustness

of the experimental study on decreased ensemble sets that we conducted, which can be improved by an iterative approach to find the optimal thresholds. We plan to incorporate sequential article data on news consumption which is absent in our methodologies that could be deficient to find the impacts of consecutive reading behaviors. Since our study focus does not fully reveal the underlying mechanism of these referral effects, future work based on social media as a holistic view may broadly expose these channels' reading charac-

teristics. To enrich the semantics of the articles, we plan to study transformer-based networks to explore the success of embeddings of the click-stream data on news outlets.

A.1. Clustering Problem

The main goal of the clustering problem is to include similar data points in the same cluster and include different data points in separated clusters (Jain et al., 1999). According to this definition, we can define the clustering problem as follows in order to get the optimal result: Given set of data with n data points in d dimensions $D = \{x_1, x_2, \dots, x_n\} \subseteq R^d$ we are in search of k number of clusters $C = \{c_1, c_2, \dots, c_k\}$ whose intersection sets are empty and represents the partitions of primary data set. As a result, each data point is expressed with a label. When comparing clusters, one of the essential consideration is that labels obtained from different clustering algorithms can give the same similarity result for data points included in the same cluster, even if they come in different permutations. Because the purpose here is to compare whether the same data points are in the same cluster or different clusters. When we observe the labels obtained from two different clustering algorithms, such as K and K' , we aim to return the similarity ratio between $[1,1,2,3,3]$ and $[3,3,1,2,2]$ to be the maximum AMI value

B.2. Internal Validation Metrics

Silhouette coefficient (S): This metric gives results between $[-1,1]$, that is how similar the data points within the cluster compared to other clusters. Higher values indicates appropriate clusters.

$$a(i) = \frac{1}{|C_i| - 1} \sum_{j \in C_i, i \neq j} d(i, j)$$

(where $d(i,j)$ is distance metric)

$$b(i) = \min_{k \neq i} \frac{1}{|C_k|} \sum_{j \in C_k} d(i, j)$$

$$Silhouette(C) = \frac{1}{|D|} \sum_{i \in D} \frac{b(i) - a(i)}{\max\{a(i), b(i)\}}$$

Dunn index-type: The value is a given ratio of inter cluster distances over intracuster diameters, where the higher values indicate the better clusters. Out of several approaches to define the diameter of the cluster, in this study we used the mean of pairwise distances in the cluster.

Assuming x and y are the data points assigned in the same cluster from the given data set D in n dimensions pairwise distances mean calculated as follows:

$$\mu = \frac{\sum_{x \in C_i} x}{|C_i|}, D_m = \frac{\sum_{x \in C_i} d(x, \mu)}{|C_i|}$$

assuming there are k clusters;

$$Dunn - Index_k = \frac{\min_{1 \leq i \leq k} \delta(C_i, C_j)}{\max_{1 \leq i \leq k} D_k}$$

Calinski Harabasz index: The index is aimed to find the ratio between cluster variance over within cluster variance, which is in the range of $[0, \infty)$. Higher values indicate good clustering.

$$CH(C) = \frac{\frac{1}{k-1} \sum_{i=1}^k ||\mu_i - \mu||^2}{\frac{1}{|D|-1} \sum_{i=1}^k \sum_{x \in C_i} ||x - \mu||^2}$$

Davies Bouldin scores: This score gives how similar of each cluster (C_i) with its most similar cluster (C_j) on average. It measures intra- and inter- cluster distances ratios. The lower values indicate appropriate clustering where it ranges between $[0, \infty)$.

When the average distance between each data point with the center of the cluster is defined as S_i and the inter cluster centroid distance is defined as $N_{i,j}$, the measurement of the goodness of cluster is $R_{i,j}$

$$R_{i,j} = \frac{S_i + S_j}{N_{i,j}}$$

and the Davies-Bouldin index is defined as:

$$Davies - Bouldin = \frac{1}{k} \sum_{i=1}^k \max_{i \neq j} R_{i,j}$$

S-Dbw (Scatter and Density between clusters) Validity Index: This metric consists of two objectives as shown in below. The first part $Scat(\#c)$ is related to the average scattering within the clusters that is obtained by partitioning the dataset. So, minimum values indicates better result in terms of compactness and the separation. The second part $Dens_bw(\#c)$ considers intra-cluster densities by comparing the clusters' center points, thus here minimum values also indicate better separation ($\#c$: Number of total clusters, C_i : i -th cluster, $\sigma(C_i)$: variance of C_i , D : Dataset, $f(x, u_{i,j})$: the midpoint of the clusters' centers as a defined line segment, $\|X\| = (X^T X)^{1/2}$)

$$Scat(\#c) = \frac{\frac{1}{\#c} \sum_{i=1}^{\#c} \|\sigma(C_i)\|}{\|\sigma(D)\|}$$

$$Dens_bw(\#c) = \frac{1}{\#c(\#c - 1)} \sum_{i=1} \left[\sum_{j \neq i} \frac{\sum_{x \in C_i \cup C_j} f(x, u_{i,j})}{\max\{\sum_x \epsilon C_i f(x, c_i), \sum_x \epsilon C_j f(x, c_j)\}} \right]$$

$$S_dbw = Scat(\#c) + Dens_bw(\#c)$$

There are other versions on S_dbw which we compare during the study. The problem with S_dbw reflected by other studies. The first drawback is, since $Dens_bw(\#c)$ in S_dbw measures neighborhood within the standard deviation, it could not cover the inter-cluster similarity especially for the non-circular clusters. Secondly, $Scat(\#c)$ part for intra-cluster similarity does not take into account tuples which might effect when there is similar variance among two cluster with difference tuple sizes.

The approach introduced by Kim et. al. ((Kim and Lee, 2003)), for the second part of the formulation, uses cluster based inter-cluster similarity by considering confidence interval for each dimension which provides to be defined the size and shape of the densities of clusters, on the other hand for intra-cluster similarity uses weighted average variance within clusters.

Tong et. al ((Tong and Tan, 2009)) points some drawbacks introduced by (Kim and Lee, 2003). Since (Kim and Lee, 2003) is not consider the discrepancy among the clusters, selecting middle point of the margin notoriously effect the center choice. For the $Scat(\#c)$ part, it points out that when cluster numbers are increasing the result of this part will be monotonically increasing as well. To overcome these, for the $Dens_bw(\#c)$ part this approach selects margin region instead of middle point of the line segment among clusters to improve inter-cluster similarity. For intra-cluster similarity. For within cluster similarity it prevents monotonically increasing values by keeping the constant although the number of clusters increasing.

C.3. External Validation Metrics

Normalized Mutual Information (NMI): In information theory, Mutual Information (MI) is defined as the amount of information obtained from one discrete-valued random variable X , by observing the other random variable Y . Assuming the joint probability distribution of two random variables is $\rho_{X,Y}$ and the expected value of this distribution is \mathbf{E}_ρ , then MI is defined as:

$$I(X, Y) = \mathbf{E}_{\rho_{X,Y}} \left[\log \frac{\rho_{X,Y}}{\rho_X \rho_Y} \right]$$

Since $I(X, Y)$ is not bounded above, normalizing it provides the results in the range of $[0, 1]$, assuming $H(X)$ and $H(Y)$ are the marginal entropies of random variables;

$$H(X) = -\mathbf{E}_{\rho_X}[\log \rho_X], I(X, Y) \leq \min(H(X), H(Y))$$

$$NMI(X, Y) = \frac{I(X, Y)}{\sqrt{H(X)H(Y)}}$$

As defined in (Strehl and Ghosh, 2002), NMI can be interpreted as the labels similarities of the clustering results, even they might come from different permutations. In this case the assumed X and Y discrete random variables can be interpreted as C , as clustered data label assignments, and C^* as ground-truth labels.

Adjusted Mutual Information (AMI): The adjustment of the result comes from MI is required, since MI values is higher when there are larger number of clusters not necessarily having more information shared among them. MI is adjusted for chance as follows (Vinh et al., 2010), which ranges between $[0, 1]$ that 1 indicates two label assignments are equal:

$$AMI(C, C^*) = \frac{I() - \mathbf{E}(I)}{\text{mean}(H(C), H(C^*)) - \mathbf{E}(I)}$$

Averaged Normalized Mutual Information: as defined in the (Helfmann et al., 2018), in a given ensemble of clusterings K , we can get the single clustering C information shared with the whole set of ensembles with the size of m , by:

$$ANMI(C, K) = \frac{1}{m} \sum_{i=1}^m NMI(C, C_i)$$

D.4. Distance Metrics

Jensen-Shannon Divergence (JSD): gives symmetric results and finite value when computing probability vectors defined as considering U and V are the vectors of different distributions. D is Kullback-Leibler divergence, and m is the mean of the vectors computed point-wise. Kullback-Leibler measures the distance between two vectors by calculating entropy, and each vector values are sum to 1:

$$Jensen - Shannon : \sqrt{\frac{D(u||m) + D(v||m)}{2}}$$

$$D_{KL}(U||M) = - \sum_{x \in X} U(x) \log \frac{M(x)}{U(x)}$$

(Menéndez et al., 1997)

References

- Akbari, E., Dahlan, H.M., Ibrahim, R., Alizadeh, H., 2015. Hierarchical cluster ensemble selection. *Engineering Applications of Artificial Intelligence* 39, 146–156.
- Alizadeh, H., Minaei-Bidgoli, B., Parvin, H., 2014. To improve the quality of cluster ensembles by selecting a subset of base clusters. *Journal of Experimental & Theoretical Artificial Intelligence* 26, 127–150.
- Aras, G., Makaroğlu, D., Demir, S., Cakir, A., 2021. An evaluation of recent neural sequence tagging models in turkish named entity recognition. *Expert Systems with Applications* 182, 115049.
- Arora, P., Varshney, S., et al., 2016. Analysis of k-means and k-medoids algorithm for big data. *Procedia Computer Science* 78, 507–512.
- Azimi, J., Fern, X., 2009. Adaptive cluster ensemble selection, in: Twenty-First International Joint Conference on Artificial Intelligence.
- Banerjee, A., Dave, R.N., 2004. Validating clusters using the hopkins statistic, in: 2004 IEEE International conference on fuzzy systems (IEEE Cat. No. 04CH37542), IEEE. pp. 149–153.
- Bar-Gill, S., Inbar, Y., Reichman, S., 2021. The impact of social vs. non-social referring channels on online news consumption. *Management Science* 67, 2420–2447.
- Benlian, A., 2015. Web personalization cues and their differential effects on user assessments of website value. *Journal of management information systems* 32, 225–260.
- Bogaard, T., Hollink, L., Wielemaker, J., Hardman, L., Van Ossenbruggen, J., 2019a. Searching for old news: User interests and behavior within a national collection, in: Proceedings of the 2019 Conference on Human Information Interaction and Retrieval, pp. 113–121.
- Bogaard, T., Hollink, L., Wielemaker, J., Hardman, L., Van Ossenbruggen, J., 2019b. Searching for old news: User interests and behavior within a national collection, in: Proceedings of the 2019 Conference on Human Information Interaction and Retrieval, pp. 113–121.
- Boongoen, T., Lam-On, N., 2018. Cluster ensembles: A survey of approaches with recent extensions and applications. *Computer Science Review* 28, 1–25.
- Calinski, T., Harabasz, J., 1974. A dendrite method for cluster analysis. *Communications in Statistics-theory and Methods* 3, 1–27.
- Castellano, G., Fanelli, A.M., Torsello, M.A., 2013. Web usage mining: discovering usage patterns for web applications, in: *Advanced Techniques in Web Intelligence-2*. Springer, pp. 75–104.
- Catledge, L.D., Pitkow, J.E., 1995. Characterizing browsing strategies in the world-wide web. *Computer Networks and ISDN systems* 27, 1065–1073.
- Chiou, L., Tucker, C., 2017. Content aggregation by platforms: The case of the news media. *Journal of Economics & Management Strategy* 26, 782–805.
- Dellarocas, C., Katona, Z., Rand, W., 2013. Media, aggregators, and the link economy: Strategic hyperlink formation in content networks. *Management science* 59, 2360–2379.
- Dunn, J.C., 1974. Well-separated clusters and optimal fuzzy partitions. *Journal of cybernetics* 4, 95–104.
- Fern, X.Z., Brodley, C.E., 2004. Solving cluster ensemble problems by bipartite graph partitioning, in: Proceedings of the twenty-first international conference on Machine learning, p. 36.
- Fern, X.Z., Lin, W., 2008. Cluster ensemble selection. *Statistical Analysis and Data Mining: The ASA Data Science Journal* 1, 128–141.
- Flaxman, S., Goel, S., Rao, J.M., 2016. Filter bubbles, echo chambers, and online news consumption. *Public opinion quarterly* 80, 298–320.
- Freedman, D., Diaconis, P., 1981. On the histogram as a density estimator: L 2 theory. *Zeitschrift für Wahrscheinlichkeitstheorie und verwandte Gebiete* 57, 453–476.
- Grech, D., Clough, P., 2016a. Investigating cluster stability when analyzing transaction logs, in: Proceedings of the 16th ACM/IEEE-CS on Joint Conference on Digital Libraries, pp. 115–118.
- Grech, D., Clough, P., 2016b. Investigating cluster stability when analyzing transaction logs, in: Proceedings of the 16th ACM/IEEE-CS on Joint Conference on Digital Libraries, pp. 115–118.
- Handl, J., Knowles, J., Kell, D.B., 2005. Computational cluster validation in post-genomic data analysis. *Bioinformatics* 21, 3201–3212.
- Helfmann, L., von Lindheim, J., Mollenhauer, M., Banisch, R., 2018. On hyperparameter search in cluster ensembles. *arXiv preprint arXiv:1803.11008*.
- Jain, A.K., Murty, M.N., Flynn, P.J., 1999. Data clustering: a review. *ACM computing surveys (CSUR)* 31, 264–323.
- Jing, L., Tian, K., Huang, J.Z., 2015. Stratified feature sampling method for ensemble clustering of high dimensional data. *Pattern Recognition* 48, 3688–3702.
- Kim, Y., Lee, S., 2003. A clustering validity assessment index, in: Pacific-Asia Conference on Knowledge Discovery and Data Mining, Springer. pp. 602–608.
- Köster, A., Matt, C., Hess, T., 2021. Do all roads lead to rome? exploring the relationship between social referrals, referral propensity and stickiness to video-on-demand websites. *Business & Information Systems Engineering* 63, 349–366.
- Kuncheva, L.I., Vetrov, D.P., 2006. Evaluation of stability of k-means cluster ensembles with respect to random initialization. *IEEE transactions on pattern analysis and machine intelligence* 28, 1798–1808.
- Li, T., Ding, C., Jordan, M.I., 2007. Solving consensus and semi-supervised clustering problems using nonnegative matrix factorization, in: Seventh IEEE International Conference on Data Mining (ICDM 2007), IEEE. pp. 577–582.
- Lin, C., Xie, R., Guan, X., Li, L., Li, T., 2014. Personalized news recommendation via implicit social experts. *Information Sciences* 254, 1–18.
- Liu, J., Dolan, P., Pedersen, E.R., 2010a. Personalized news recommendation based on click behavior, in: Proceedings of the 15th international conference on Intelligent user interfaces, pp. 31–40.
- Liu, Y., Li, Z., Xiong, H., Gao, X., Wu, J., 2010b. Understanding of internal clustering validation measures, in: 2010 IEEE international conference on data mining, IEEE. pp. 911–916.
- Makaroğlu, D., Çakır, A., Kocabaş, K., 2019. Social media and clickstream analysis in turkish news with apache spark, in: International Conference on Intelligent and Fuzzy Systems, Springer. pp. 221–228.
- Mao, E., Zhang, J., 2015. What drives consumers to click on social media ads? the roles of content, media, and individual factors, in: 2015 48th Hawaii International Conference on System Sciences, IEEE. pp. 3405–3413.
- McConville, R., Santos-Rodríguez, R., Piechocki, R.J., Craddock, I., 2021. N2d(not too) deep clustering via clustering the local manifold of an autoencoded embedding, in: 2020 25th International Conference on Pattern Recognition (ICPR), IEEE. pp. 5145–5152.
- McInnes, L., Healy, J., Astels, S., 2017. hdbscan: Hierarchical density based clustering. *Journal of Open Source Software* 2, 205.
- McInnes, L., Healy, J., Melville, J., 2020. Umap: uniform manifold approximation and projection for dimension reduction.
- Menéndez, M., Pardo, J., Pardo, L., Pardo, M., 1997. The jensen-shannon divergence. *Journal of the Franklin Institute* 334, 307–318.
- Möller, J., van de Velde, R.N., Merten, L., Puschmann, C., 2020. Explaining online news engagement based on browsing behavior: Creatures of habit? *Social Science Computer Review* 38, 616–632.
- Pividori, M., Stegmayer, G., Milone, D.H., 2016. Diversity control for improving the analysis of consensus clustering. *Information Sciences* 361, 120–134.
- Rodríguez-Fernández, V., Menéndez, H.D., Camacho, D., 2017. A study on performance metrics and clustering methods for analyzing behavior in uav operations. *Journal of Intelligent & Fuzzy Systems* 32, 1307–1319.
- Rousseeuw, P.J., 1987. Silhouettes: a graphical aid to the interpretation and validation of cluster analysis. *Journal of computational and applied*

- mathematics 20, 53–65.
- Schubert, E., Sander, J., Ester, M., Kriegel, H.P., Xu, X., 2017. Dbscan revisited, revisited: why and how you should (still) use dbscan. *ACM Transactions on Database Systems (TODS)* 42, 1–21.
- Strehl, A., Ghosh, J., 2002. Cluster ensembles—a knowledge reuse framework for combining multiple partitions. *Journal of machine learning research* 3, 583–617.
- Su, Q., Chen, L., 2015. A method for discovering clusters of e-commerce interest patterns using click-stream data. *electronic commerce research and applications* 14, 1–13.
- Thorson, K., Wells, C., 2016. Curated flows: A framework for mapping media exposure in the digital age. *Communication Theory* 26, 309–328.
- Tong, J., Tan, H., 2009. Clustering validity based on the improved s_{dbw}^* index. *Journal of Electronics (China)* 26, 258–264.
- Varia, J., Mathew, S., et al., 2014. Overview of amazon web services. *Amazon Web Services* 105.
- Vinh, N.X., Epps, J., Bailey, J., 2010. Information theoretic measures for clusterings comparison: Variants, properties, normalization and correction for chance. *The Journal of Machine Learning Research* 11, 2837–2854.
- Wang, G., Konolige, T., Wilson, C., Wang, X., Zheng, H., Zhao, B.Y., 2013. You are how you click: Clickstream analysis for sybil detection, in: 22nd {USENIX} Security Symposium ({USENIX} Security 13), pp. 241–256.
- Wang, G., Zhang, X., Tang, S., Zheng, H., Zhao, B.Y., 2016. Unsupervised clickstream clustering for user behavior analysis, in: *Proceedings of the 2016 CHI conference on human factors in computing systems*, pp. 225–236.
- Wegmann, M., Zipperling, D., Hillenbrand, J., Fleischer, J., 2021. A review of systematic selection of clustering algorithms and their evaluation. *arXiv preprint arXiv:2106.12792*.
- Wells, C., Thorson, K., 2017. Combining big data and survey techniques to model effects of political content flows in facebook. *Social Science Computer Review* 35, 33–52.
- Xu, J., Forman, C., Kim, J.B., Van Ittersum, K., 2014. News media channels: Complements or substitutes? evidence from mobile phone usage. *Journal of Marketing* 78, 97–112.
- Yanatma, S., 2018. Reuters institute digital news report 2018–turkey supplementary report.
- Yang, F., Li, T., Zhou, Q., Xiao, H., 2017. Cluster ensemble selection with constraints. *Neurocomputing* 235, 59–70.
- Yeo, I.K., Johnson, R.A., 2000. A new family of power transformations to improve normality or symmetry. *Biometrika* 87, 954–959.
- Zhang, J., Kamps, J., 2010. Search log analysis of user stereotypes, information seeking behavior, and contextual evaluation, in: *Proceedings of the third symposium on Information interaction in context*, pp. 245–254.
- Zheng, L., Li, L., Hong, W., Li, T., 2013. Penetrate: Personalized news recommendation using ensemble hierarchical clustering. *Expert Systems with Applications* 40, 2127–2136.